

Optical-Switch Benes Architecture based on 2-D MEMS

Guido Maier*, Luigi Savastano*[†], Achille Pattavina[‡], Stefano Bregni[‡] and Mario Martinelli*[‡]

*CoreCom - Milan, Italy. Email: {maier,martinelli}@corecom.it

[‡]DEI, Politecnico di Milano - Milan, Italy. Email: {pattavina,bregni}@elet.polimi.it

[†]now with DVT Pirelli Broadband Solutions - Milan, Italy. Email: luigi.savastano@pirelli.com

Abstract—This paper¹ presents a novel implementation scheme of the Benes network based on the 2-D MEMS technology. A recursive design procedure is proposed defining the switch geometry for any optical port-count. An analytical approach is adopted to provide a scalability evaluation of the architecture based upon basic parameters such as number of mirrors, substrate area, longest optical path and highest number of reflections.

I. INTRODUCTION

Micro-Electro-Mechanical Systems (MEMS) technology [1] emerged as one of the most promising among several candidates ([2]–[6]) for a future large-scale development of optical switching matrices, due to MEMS feature of combining the merits of free-space optics (low crosstalk and loss) with the compactness of integrated micro-metric silicon devices. In this paper we propose a new architecture for implementing the Benes network [7] by 2-D MEMS. We will refer to this new Rearrangeable Non-Blocking (RNB) Banyan-based network [8] by the name MEMS-Benes Network (MBN). Compared to other alternative architectures (*Crossbar*, *L-Switching matrix* [9], [10], *Array Interconnection* [11]) the Benes network allows to achieve good loss uniformity (*differential loss*) and low number of reflections with a small number of active Switching Elements (SEs), asymptotically increasing as $O[N \log_2(N)]$ (to be compared to the $O[N^2]$ of the Crossbar). The implementation does not require to tilt mirrors at a large number of different angles, as in a recently proposed 2-D MEMS implementations of the Benes architecture [12]. On the contrary, in order to simplify the fabrication process and reduce the tolerance constraints on mirror alignment, the proposed design approach is such that all the mirrors are oriented along only two orthogonal directions and are located on a regular grid on the substrate. The generic MBN with N inlets and outlets is designed according to the recursive procedure presented in the following sections. Sec. II describes the elementary 4×4 basis of the recursion. Sec. III is dedicated to the 8×8 and 16×16 MBNs, which are designed according to special rules, slightly different from the general procedure. Such general procedure, holding for any $N \times N$ MBN with $N \geq 32$, is presented in Sec. IV, while in Sec. V the main complexity parameters of the MBNs are analyzed.

¹This work was partially supported by MIUR, Italy, under PRIN Project OSATE.

II. ELEMENTARY 4×4 MEMS-BENES ARCHITECTURE

It is well known from the “classical” switching-network theory [7], [8] that the Benes network has a recursive construction rule. For instance, the 16×16 Benes is built starting from two 8×8 Benes networks and adding an extra input and an extra output Banyan symmetrical stages (see Fig. 1). In general, the $N \times N$ Benes is implemented combining two $(N/2) \times (N/2)$ Benes with two extra symmetrical Banyan stages.

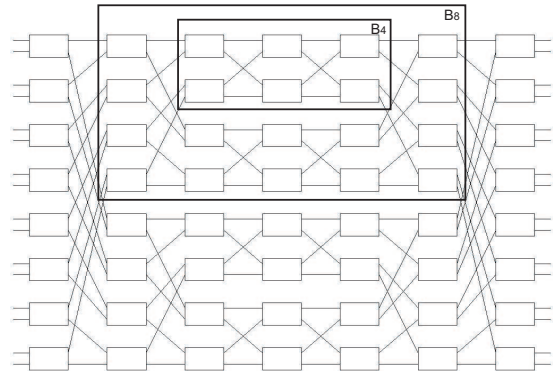


Fig. 1. 16×16 Benes architecture. In order to remark the recursive construction procedure, one of the 8×8 Benes block (B8) of the 16×16 network has been highlighted; the 8×8 block is in turn built starting from the basic 4×4 block (B4).

This general property of the Benes architecture is a fundamental enabler to develop the MEMS implementation here described, which is based on a recursive scalable design approach. The elementary MBN block, the starting architecture from which a MBN of any size can be obtained by recursion, is the 4×4 switch, represented in Fig. 2.

The figure also depicts the functionally equivalent Benes network, according to the classical representation. The MEMS device is seen from the above the substrate: the electro-mechanical micro-mirrors are represented by segments corresponding to their vertical position. The optical beams enter the switch from the left side and free-space propagate in a plane parallel to the substrate. Mirrors are all oriented so that the reflecting plane of each makes a 45° angle with the propagation direction of the optical beam: thus beams are right-angle deflected upon each reflection.

The optical beams all leave the switch from the right side. The six 2×2 switching elements (labelled from A to F) are

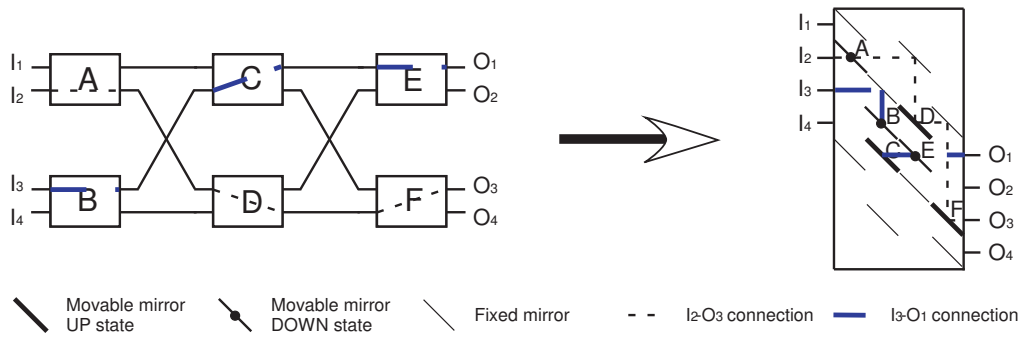


Fig. 2. 4×4 MEMS-Benes network: the elementary block. The optical paths of two connections are displayed.

implemented in the MBN by six Movable Mirrors (MMs). A bi-univocal correspondence can be established between SE and MM states which can be maintained for all the mirrors and for MBNs of any size. The *bar* SE state corresponds to the laying-down position of the mirror (mirror set parallel to the substrate and not interfering with the beam); the *cross* SE state corresponds to the tilted-up position of the MM (reflecting surface orthogonal to the substrate and deviating a beam). The MBN also contains Fixed Mirrors (FMs) (represented by a thin segment in the figures): these mirrors have the purpose of steering the beams towards specific locations of the switch, for example steering them to leave the device from the same side and in the correct order.

The one-to-one correspondence between SEs and MMs allows the connection routing algorithms to be adopted inside the MBN to be very simply inferred from the algorithms developed for the traditional Benes network. Given an input-output permutation requested to the MBN, the well-known *looping algorithm*, derived from the classical Benes representation, can be applied to decide the state of each SE. The state of the micro mirror in the MBN is then simply set according to the state of its corresponding SE in the classical Benes. Fig. 2 shows an example of routing across the 4×4 MBN: there are two connections requested, one from I_2 to O_3 and the other from I_3 to O_1 . The 4×4 Benes is also represented according to the classical method, supporting the same connections: the functional correspondence between MSN-MMs and SEs is clear.

To support the particular design approach described in the next section, we introduce here a variation of the 4×4 MBN. Let us name the architecture displayed in Fig. 2 a *vertical* 4×4 MBN. A *horizontal* 4×4 MBN is also needed to complete the recursive construction procedure. It should be noted that in the 4×4 MBN defined above mirrors (both movable and fixed ones) are placed in specific locations of a regular grid: each mirror can be thought as being inscribed into a square box of the grid (a virtual “*tile*”) and in its upright position is aligned with the diagonal of such a box. It is therefore possible to describe the switch topology by a matrix. The element (i, j) of such matrix is (conventionally) zero, one or two if the $(i$ th-vertical, j th-horizontal) square tile of the substrate (counting

from the top-left corner) has nothing, a fixed or a movable mirror, respectively, along its diagonal. In particular, the grid of the vertical 4×4 MBN has 8 rows and 4 columns of tiles.

This matrix-equivalent representation is available not only for the 4×4 case, but for all the MBNs. Thus, in general, given a *vertical* $N \times N$ MBN whose topology is described by the matrix \mathbf{T} , its *horizontal* version is described by the transpose \mathbf{T}' (*vertical-to-horizontal transformation*). The dual property obviously holds for the *horizontal-to-vertical transformation*. The orientation of all the mirrors relative to an absolute reference direction does not change in the vertical-horizontal (horizontal-vertical) transformation, while the beam-propagation direction is turned of 90° . So, in a vertical MBN the main propagation direction is from the left to the right side, while in a horizontal MBN propagation mainly occurs from the top to the bottom side. Let us note that, unless otherwise explicitly specified, we will always assume vertical MBNs in the following.

III. 8×8 AND 16×16 MEMS-BENES NETWORKS

Let us consider the already mentioned recursive construction of the Benes. In particular, the 8×8 network is obtained by interconnecting two 4×4 Benes subnetworks with two symmetrical input and output Banyan stages (see Fig. 1 again). Each one of these two extra stages includes four SEs. In order to distinguish the two $(N/2) \times (N/2)$ Benes subnets which compose a $N \times N$ Benes, we name \mathcal{A} the top one and \mathcal{B} the bottom one, respectively. Each SE of the first and last extra-stages is connected to both the subnets in an orderly way. This means that the topmost SE of the first stage is connected to the topmost inlets of the two subnets, the second topmost to the second topmost inlets, and so on, until the bottommost SE, connected to the $N/2$ -th inlets of both the subnets². The same holds symmetrically for the output extra stage. The construction of an 8×8 MBN, in its *vertical* version (Fig. 3), is thus quite straightforward: we need one vertical and one horizontal 4×4 MBN, which will play the roles of subnet \mathcal{B} and \mathcal{A} , respectively.

²The interconnection pattern is a *h-unshuffle* σ_h^{-1} , with $h = \log_2 N - 1$ [8].

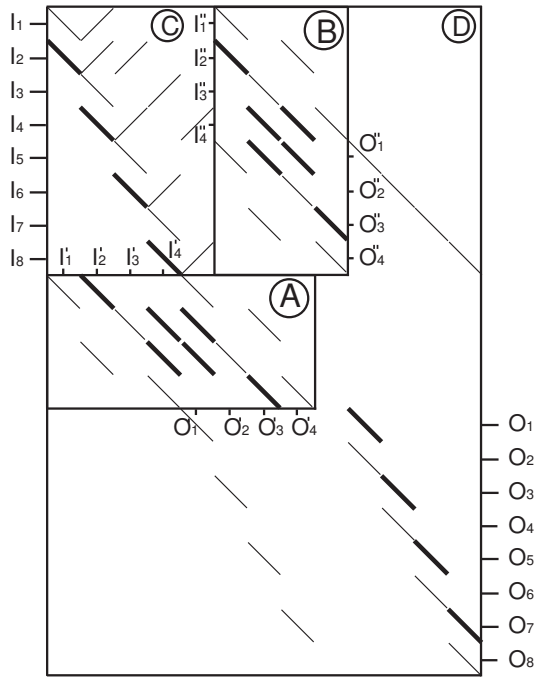


Fig. 3. 8×8 MEMS-Benes network (vertical version).

The two input and output extra-stages are implemented by adding other micro mirrors on the substrate hosting the two 4×4 MBNs. The region \mathcal{C} (\mathcal{D}) groups the micro mirrors corresponding to the input (output) stage of the 8×8 MBN. This grouping holds for any $N \times N$ MBNs with $N \geq 8$ and thus the \mathcal{C} and \mathcal{D} regions will always contain from now on the components corresponding to the SEs of the first and last stages of a Benes network in its classical representation and their respective interconnection links.

All the input optical beams reaches the MMs of region \mathcal{C} . According to the states of these elements the beams are then steered to either the subnet \mathcal{A} or the subnet \mathcal{B} . The optical outputs from both the subnets are collected by the MMs placed in region \mathcal{D} , which are responsible to deflect each beam to the correct final output port.

Differently from the 4×4 MBN, in the 8×8 architecture mirrors have two possible orientations ($\pm 45^\circ$) referred to the propagation direction of beams. Moreover, optical signals do not travel any more in only two possible directions (top to bottom and left to right), but in some segments of the optical path they are allowed to propagate also in the bottom-to-top direction. Such scheme has some drawbacks: not only the physical implementation is slightly more complicated, but also the mean propagation length of the beams inside the switch is increased, thus increasing the loss. These drawbacks are however the consequence of having conceived this specific 8×8 MBN design with the target of minimizing the substrate-area occupation (to which many properties are strongly related).

The correspondence of the first-stage SEs of the 8×8 Benes with the MMs of the \mathcal{C} region in the MBN follows a general rule which holds for any $N \times N$ MBN. The movable mirror

corresponding to the k -th SE of the first stage ($1 \leq k \leq N/2$, numbering the SEs starting from the top one) is placed in the $(2k)$ -th row of the MBN. Analogously, the movable mirror corresponding to the k -th SE of the last stage is placed in the $(2k + 1)$ row of the MBN.

From the vertical 8×8 MBN its *horizontal* version can be easily derived by applying the vertical-to-horizontal transformation rule (see Sec. II). The resulting architecture is depicted in Fig. 4.

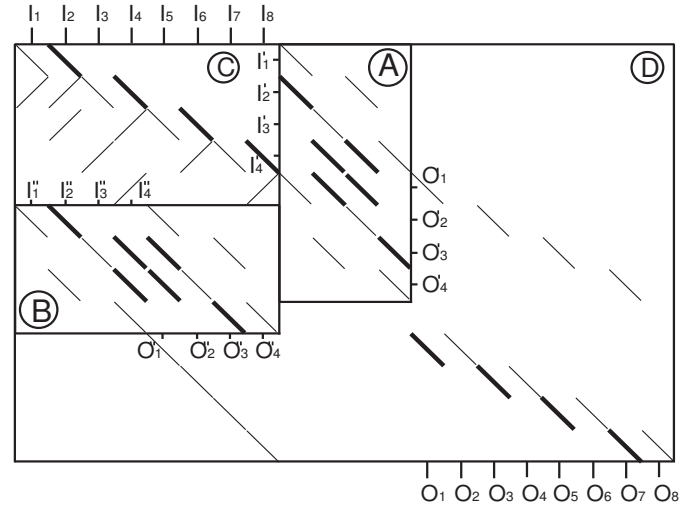


Fig. 4. 8×8 MEMS-Benes network (horizontal version).

The 16×16 MBN is built using the two vertical and horizontal 8×8 MBNs plus other micro mirrors in the \mathcal{C} and \mathcal{D} regions for the input and output stages. Like in the 8×8 case, four mirrors are required in the \mathcal{C} region (in the \mathcal{D} region) for each pair of adjacent inlets (outlets) of the architecture. Only one of these four micro mirrors is an MM. The substrate-area utilization in the \mathcal{C} and \mathcal{D} regions is quite low: this is a feature common to all the MBNs implemented according to our design rule with size $N > 4$.

IV. $N \times N$ MEMS-BENES WITH $N \geq 32$

Let us provide a general design rule for all the $N \times N$ MBN architectures having a number of optical inlets and outlets $N \geq 32$. The procedure applied to the *vertical* version of the $N \times N$ MBN will be described in details.

The physical overall horizontal and vertical dimensions of a MBN are named by $H_{BM}(N)$ and $V_{BM}(N)$, respectively. These parameters are normalized by the *pitch* length, i.e. the distance between the centers of two neighbor micro mirrors, assuming an “isotropic” distribution of the mirrors over the substrate. The pitch is incidentally equal to the length of the side of the square tiles inscribing the mirrors. The pitch length in physical units of measurement is determined by implementation factors such as mirror dimension and fabrication-process requirements (space needed to accommodate the mirror struc-

ture and its driving device)³.

As explained above, a $N \times N$ MBN requires a vertical and a horizontal $(N/2) \times (N/2)$ MBNs as building blocks. The left margin of the vertical $(N/2) \times (N/2)$ MBN (the \mathcal{B} subnet) is at a distance $V_{\text{BM}}(N/2) - H_{\text{BM}}(N/2)$ from the left margin of the overall substrate. The top margin of the horizontal $(N/2) \times (N/2)$ MBN (the \mathcal{A} subnet) is at a distance $V_{\text{BM}}(N/2)$ from the top margin of the overall substrate. This location of the two subnets on the substrate allows to have the two subnets adjacent side-to-side, perfectly aligning the right margin of \mathcal{A} to the right margin of \mathcal{B} .

The reader may wonder at this point why the 8×8 and 16×16 MBNs are not included under the general rule. It can be noticed that as N decreases the fraction of the longer side of the MBN occupied by the optical inlets and outlets gets larger, reaching a maximum of 50% in the 4×4 case. In the 8×8 and 16×16 MBNs the subnets (i.e. the 4×4 and the 8×8 MBN, respectively) can not be aligned on the left, as described above for the $N \geq 32$ case, because otherwise one of the two subnets would “mask” the inlets of the other one. This is the reason why we had for these two cases to develop the two *ad hoc* design procedures described in Sec. III, which are slightly different from the general rule, but allows to achieve in any case a limited occupied substrate surface.

After having defined the placement of the two subnets \mathcal{A} and \mathcal{B} with size $N/2$ we have to define position and orientation of all the the micro mirrors of the \mathcal{C} and \mathcal{D} regions. In the MEMS scheme introduced in Sec. II the values $\{0, 1, 2\}$ of element $t_{i,j}$ of matrix \mathbf{T} indicate that the corresponding virtual tile in the substrate hosts nothing, a FM or a MM, respectively. Tiles are numbered starting from the top-left corner; rows go from 1 to $V_{\text{BM}}(N)$ and columns from 1 to $H_{\text{BM}}(N)$. Since not all the mirrors are actually oriented in the same direction, let us slightly modify the definition of \mathbf{T} by introducing a sign for the non-zero elements. Consider a beam propagating in the left-to-right direction. A positive (negative) sign conventionally indicates a mirror oriented so to deflect that beam towards the top (bottom) side of the substrate.

Let us now consider a pair of adjacent inlets I_{2k-1} and I_{2k} with $k = 1, 2, 3, \dots, N/2$. In the region \mathcal{C}

- $t_{i,j} = -1$ with $i = 2k - 1$ and $j = k$;
- $t_{i,j} = -2$ with $i = 2k$ and $j = k$;
- $t_{i,j} = +1$ with $i = 2k$ and $j = k + 1$;
- $t_{i,j} = +1$ with $i = k$ and $j = k + 1$.

Analogously, in the \mathcal{D} region, for each pair of adjacent outlets O_{2k-1} and O_{2k} ($k = 1, 2, 3, \dots, N/2$)

- $t_{i,j} = -1$ with $i = y - z + k$ and $j = y + k$
- $t_{i,j} = -2$ with $i = y + x + 2k - 1$ and $j = y + k$
- $t_{i,j} = -1$ with $i = y + x + 2k - 1$ and $j = y - z + k$
- $t_{i,j} = -1$ with $i = y + x + 2k$ and $j = y + k$

where: $z = N/2$, $x = H_{\text{BM}}(z)$ and $y = V_{\text{BM}}(z)$.

³A (rather conservative) typical value is, for example, $(3R+800)/\sqrt{2}$ μm , where R , the mirror radius, typically ranges from 200 to 400 μm [13].

Three FMs and one MM are thus needed for any pair of adjacent inlets (outlets) in the region \mathcal{C} (\mathcal{D}). Optical inlets are located on the left side of the switch, occupying the first N rows, while the outlets are located on the right side occupying the last N rows. Region \mathcal{C} comprises $3N/2$ FMs and $N/2$ MMs, and the same holds for region \mathcal{D} .

We should finally add that the *horizontal* $N \times N$ MBN can be obtained from the vertical MBN by applying the vertical-to-horizontal transformation $\mathbf{T}_H = \mathbf{T}'$. A positive (negative) element of \mathbf{T}_H indicates a mirror deflecting a beam propagating in the top-bottom direction towards the right (left). Figures representing $N \times N$ MEMS-Benes with $N \geq 8$ are too large to fit into the limited length of this paper and will be provided during the oral presentation.

V. BASIC FEATURE EVALUATION

The topological design of the MBNs for any number of inlets and outlets has been so far described. Let us now calculate the parameters that characterize the novel proposed architecture and which would be most relevant for a complete physical performance evaluation. The following sections provide the equations expressing the parameters as functions of the switch port-count.

The first parameters to evaluate are those related to the overall physical dimensions of the MBNs, which are: substrate lateral sizes $H_{\text{BM}}(N)$ and $V_{\text{BM}}(N)$ (introduced in Sec. IV) and substrate area $A_{\text{BM}}(N) = H_{\text{BM}}(N) \cdot V_{\text{BM}}(N)$. Let us consider the general case of a (vertical) $N \times N$ MBN with $N \geq 32$. The vertical size must be sufficient to accommodate: a long side of a vertical $(N/2) \times (N/2)$ MBN, a short side of an horizontal $(N/2) \times (N/2)$ MBN, the N outlets of the network. Horizontally, the long side of the horizontal $(N/2) \times (N/2)$ MBN plus the $N/2$ mirrors of the \mathcal{D} region has to be accommodated. The following recursive function of $V_{\text{BM}}(N)$ descends

$$V_{\text{BM}}(N) = (5/4)N + V_{\text{BM}}(N/2) + V_{\text{BM}}(N/4)$$

The solution is

$$V_{\text{BM}}(N) = c_1 k_1^{\log_2 N} + c_2 k_2^{\log_2 N} + 5N \quad (1)$$

where: $k_1 = [(1 + \sqrt{5})/2]$, $k_2 = [(1 - \sqrt{5})/2]$ and c_1 and c_2 are two coefficients that must be determined by imposing the initial conditions. These are given by the two values, calculated by inspection: $V_{\text{BM}}(32) = 111$ and $V_{\text{BM}}(64) = 240$.

By a similar procedure a closed-form equation can be found also for $H_{\text{BM}}(N)$

$$H_{\text{BM}}(N) = (c_1/k_1)k_1^{\log_2 N} + (c_2/k_2)k_2^{\log_2 N} + 3N \quad (2)$$

From Eq. 1 and 2 the computation of $A_{\text{BM}}(N)$ is trivial.

Let us now evaluate the number of micro mirrors needed to implement an $N \times N$ MBN: this is an important cost parameter, especially when movable mirrors are considered. As underlined in Sec. II, each 2×2 SE of the Benes network in its “classical” representation corresponds one-to-one to a MM of the MBN. Therefore the number of movable micro

TABLE I
MBN PHYSICAL PARAMETERS.

N	$V_{\text{BM}}(N)$	$H_{\text{BM}}(N)$	$A_{\text{BM}}(N)$	MM_{BM}	FM_{BM}	TM_{BM}	$LP_{\text{BM}}(N)$	$MRN_{\text{BM}}(N)$
4	8	4	32	6	8	14	11	6
8	20	13	260	20	40	60	34	12
16	49	30	1470	56	128	184	88	18
32	111	65	7215	144	352	496	201	24
64	240	143	34320	352	896	1248	440	30
<i>128</i>	<i>511</i>	<i>304</i>	<i>155344</i>	<i>832</i>	<i>2176</i>	<i>3008</i>	<i>936</i>	<i>36</i>
<i>256</i>	<i>1071</i>	<i>639</i>	<i>684369</i>	<i>1920</i>	<i>5120</i>	<i>7040</i>	<i>1959</i>	<i>42</i>

mirrors $MM_{\text{BM}}(N)$ in an MBN is equal to the well-known number of SEs of a Benes network

$$MM_{\text{BM}}(N) = (2 \log_2 N - 1)N/2 \quad (3)$$

The number of fixed mirrors $FM_{\text{BM}}(N)$ can be instead evaluated as follows. By inspecting Fig. 2, $FM_{\text{BM}}(4)$ of the elementary 4×4 MBN is 8. The 8×8 MBN has 12 FMs in each one of the \mathcal{C} and \mathcal{D} regions, and 8 FMs in each one of the \mathcal{A} and \mathcal{B} subnets, for a total of 40 FMs. In the general case, we can recall that in the regions \mathcal{C} and \mathcal{D} 3 FMs are needed for each pair of adjacent inlets and outlets. Thus

$$FM_{\text{BM}}(N) = 3N/2 + 2FM_{\text{BM}}(N/2) + 3N/2 \quad (4)$$

The closed-form equation is obtained by recursively developing the above equation and imposing the initial conditions ($FM_{\text{BM}}(4) = 8$)

$$FM_{\text{BM}}(N) = (3 \log_2 N - 4)N \quad (5)$$

The next two parameters are the maximum optical-path length inside the switch $LP_{\text{BM}}(N)$ and the maximum number of reflections a beam can undergo $MRN_{\text{BM}}(N)$. Both are necessary to measure the maximum optical loss (insertion loss) of the switch: this parameter is the combination of several components related to various degradation effects (further details can be found in Ref. [14]). One component is loss due to beam divergence, which is strictly dependent on the optical path length. Other components are the mirror misalignment and mirror absorption, which instead depend upon the number of reflections.

LP_{BM} for the general MBN is evaluated by adopting a recursive approach. In the 4×4 MBN beams can travel only “monotonically” in the left-right and top-bottom directions. Therefore the longest path is the one connecting the geometrically farthest inlet-outlet pair, i.e. $I_1 - O_4$. By inspection, $LP_{\text{BM}}(4) = 11$ (length normalized by the pitch). It should be noted that this is equal to the full semi-perimeter of the switch minus one pitch (the corner-tile should be not counted twice). This property can be extended to any switch with mirrors all angled at 45° with the beam propagation direction and in the same direction, where beams can propagate only parallel to the substrate sides. In the $N \times N$ MBN case, therefore, the “ideal” maximum path length we would have if all the mirrors were equally oriented is $LP_{\text{BM}}^*(N) = V_{\text{BM}}(N) + H_{\text{BM}}(N) - 1$. With $N > 4$ the longest-path evaluation is more difficult, as beams

can change their propagation direction by 180° on some path segments inside the region \mathcal{C} . It can be proved that for any $N \times N$ MBN with $N \geq 8$ the maximum path length can be computed starting from $LP_{\text{BM}}^*(N)$ and summing to it a term that accounts for all the switchbacks that the beam undergoes in the \mathcal{C} regions of all the subnets nested into the $N \times N$ MBN. Following the proof of the property (omitted here for brevity) and applying some math, the final equation to compute LP_{BM} is

$$LP_{\text{BM}}(N) = LP_{\text{BM}}^*(N) + N - 6 \quad (6)$$

It should be also added that, for the same reasoning which led to Eq. 6, the maximum-length path in all the $N \times N$ MBNs with $N \geq 8$ is always the one connecting the inlet $N - 1$ to the outlet N .

Let us now evaluate the maximum number of reflections. For the 4×4 MBN, along the worst-case connections (e.g. inlet 1 to outlet N) the beams are reflected 6 times; thus: $MRN_{\text{BM}}(4) = 6$.

For $N \times N$ MBNs with $N > 4$ the worst-case connections are always those crossing the subnet \mathcal{B} . Beams crossing \mathcal{B} accumulate a maximum of 4 reflections in region \mathcal{C} and 2 reflections in region \mathcal{D} . There always is at least one worst-case connection across the subnet \mathcal{B} which also meets the maximum number of reflections in both \mathcal{C} and \mathcal{D} . Therefore, the following recursive equation can be written

$$MRN_{\text{BM}}(N) = 6 + MRN_{\text{BM}}(N/2) \quad (7)$$

By imposing the initial condition $MRN_{\text{BM}}(4) = 6$ we obtain

$$MRN_{\text{BM}}(N) = 6(\log_2 N - 1) \quad (8)$$

It can be proved that in MBNs the longest path does not coincide with the path with most reflections, thus alleviating the combination of divergence and reflection-related effects in the maximum-loss path.

The equations in this section have been used to compute the values of all the parameters for the values of N reported in Tab. I. The rows appearing in italic in this table (as in the following ones) concerns MBNs which are actually at present hardly feasible, given their size and the current limitations on the maximum substrate area achievable by a single silicon wafer. Data for these MBNs have been nevertheless reported for theoretical completeness. In the table, $TM_{\text{BM}}(N) = MM_{\text{BM}}(N) + FM_{\text{BM}}(N)$ is the total number of micro mirrors.

VI. CONCLUDING REMARKS

A novel implementation scheme of the Benes network has been proposed based on the 2-D MEMS technology. A recursive design algorithm has been described. The standard looping algorithm applicable to the classical Benes can be adopted for connection routing and switch management also in the MEMS implementation, thanks to the one-to-one correspondence between switching mirrors and Benes switching elements. The main physical parameters of the MEMS-Benes architecture (size, substrate-area occupation, number of micro mirrors, maximum optical-path length, maximum number of reflections) have been analyzed. The study highlighted the main advantage achievable with the new MEMS Benes implementation, i.e. a very good scalability in terms of number of movable mirrors. The parameter analysis showed that the MEMS-Benes feasibility is compatible with the current 2-D MEMS technology at least up to a port-count of 64, for which the MEMS Benes requires more than 11 times less switching mirrors than the Crossbar. The Benes architecture is rearrangeable non-blocking: thus the 2-D based implementation proposed in this paper is suitable to be adopted in networks where connection rearrangements cause acceptable performance degradation. A possible application of the 2-D MBN is the implementation of the space-switching subsystem of the Optical Cross-Connect (OXC) for the Optical Transport Network (OTN). OTNs are lightpath (circuit) switched networks: in the current service scenario most of the very-large bandwidth optical connections are permanent or quite seldom reconfigured; moreover the switching speed of the nodes is not an issue (i.e. a switching response in the range of the milliseconds is still negligible compared to the total time taken for the network management system to signal reconfiguration instructions to the nodes). In such conditions, then, unfrequent OXC rearrangements carried out at a switching speed compatible with the 2-D MBN would lead to just a moderate and acceptable network unavailability increase.

REFERENCES

- [1] L.-Y. Lin, E. L. Goldstein, and R. W. Tkach, "Free-Space Micromachined Optical Switches for Optical Networking," *Journal of Selected Topics in Quantum Electronics*, vol. 5, no. 1, pp. 4–9, January-February 1999.
- [2] A. Dugan, L. Lightworks, and J. C. Chiao, "The optical switching spectrum: A primer on wavelength switching technologies," *Telecommun. Magazine*, May 2001.
- [3] A. Ware, "New photonic-switching technology for all-optical networks," *Lightwave*, pp. 92–98, March 2000.
- [4] S. Hardy, "Liquid-crystal technology vies for switching applications," *Lightwave*, pp. 44–46, December 1999.
- [5] D. A. Smith, A. Alessandro, J. E. Baran, D. J. Fritz, J. L. Jackel, and R. S. Chakravarthy, "Multiwavelength performance of an adoped acoust-optic switch," *Journal of Lightwave Technology*, vol. 14, pp. 2044–2051, September 1996.
- [6] D. K. Cheng, Y. Liu, and G. J. Sonek, "Optical switch based on thermally-activated dye-doped biomolecular thin films," *IEEE Photon. Technol. Lett.*, vol. 7, pp. 366–369, April 1995.
- [7] V. E. Benes, *Mathematical Theory of Connecting Networks and Telephone Traffic*. New York: Academic Press, 1965.
- [8] A. Pattavina, *Switching Theory: Architectures and Performance in Broadband ATM Networks*, 1st ed. Baffin Lane, Chichester, West Sussex, England: John Wiley & Sons, 1998.

- [9] T. W. Yeow, K. L. E. Law, and A. A. Goldenberg, "SOI-Based 2-D MEMS L-Switching Matrix for Optical Networking," *Journal of Selected Topics in Quantum Electronics*, vol. 9, no. 2, pp. 603–613, March-April 2003.
- [10] —, "Micromachined L-Switching Matrix," in *IEEE International Conference on Communications*, vol. 5, April-May 2002, pp. 2848–2854.
- [11] T. Y. Chai, T. H. Cheng, S. K. Bose, C. Lu, and G. Shen, "Array Interconnection for Rearrangeable 2-D MEMS Optical Switch," *Journal of Lightwave Technology*, vol. 21, no. 5, pp. 1134–1140, May 2003.
- [12] C. Y. Li, G. M. Li, V. O. K. Li, P. K. A. Wai, H. Xie, and X. C. Yuan, "Using 2×2 switching modules to build large 2-D MEMS optical switches," in *Global Telecommunications Conference*, vol. 5, December 2003, pp. 2798–2802.
- [13] L.-Y. Lin, E. L. Goldstein, and R. W. Tkach, "On the Expandability of Free-Space Micromachined Optical Cross Connects," *Journal of Lightwave Technology*, vol. 18, no. 4, pp. 482–489, April 2000.
- [14] L. Savastano, G. Maier, A. Pattavina, and M. Martinelli, "Physical-parameter design in 2-D MEMS optical switches," *Journal of Lightwave Technology*, vol. 23, no. 10, pp. 3147–3155, October 2005.